Unilamellar Nanosheet of Layered Manganese Cobalt Nickel Oxide and Its Heterolayered Film with Polycations

Eun-Jin Oh,[†] Tae Woo Kim,[†] Kyung Min Lee, Min-Sun Song, Ah-Young Jee, Seung Tae Lim, Hyung-Wook Ha, Minyung Lee, Jin-Ho Choy, and Seong-Ju Hwang*

Center for Intelligent Nano-Bio Materials (CINBM), Department of Chemistry and Nano Sciences, Ewha Womans University, Seoul 120-750, Korea. [†]These two authors contributed equally to this work.

ABSTRACT The exfoliation of layered $Li[Mn_{1/3}Co_{1/3}Ni_{1/3}]O_2$ into individual monolayers could be achieved through the intercalation of quaternary tetramethylammonium (TMA^+) ions into protonated metal oxide. An effective exfoliation occurred when the TMA^+/H^+ ratio was 0.5—50. Reactions outside this range produced no colloidal suspension, but all the manganese cobalt nickel oxides precipitated. Atomic force microscopy and transmission electron microscopy clearly demonstrated that exfoliated manganese cobalt nickel oxide nanosheets have a nanometer-level thickness, underscoring the formation of unilamellar nanosheets. The maintenance of the hexagonal atomic arrangement of the manganese cobalt nickel oxide layer upon the exfoliation was confirmed by selected area electron diffraction analysis. According to diffuse reflectance ultraviolet—visible spectroscopy, the exfoliated manganese cobalt nickel oxides displayed distinct absorption peaks at ~354 and ~480 nm corresponding to the d—d transitions of octahedral metal ions, which contrasted with the featureless spectrum of the pristine metal oxide. In the light of zeta potential data showing the negative surface charge of manganese cobalt nickel oxide nanosheets, a heterolayered film of manganese cobalt nickel oxide and conductive polymers could be prepared through the successive coating process with colloidal suspension and polycations. The UV—vis and X-ray diffraction studies verified the layer-by-layer ordered structure of the obtained heterolayered film, respectively.

KEYWORDS: layered manganese cobalt nickel oxide · exfoliation · nanosheets · colloidal suspension · heterolayered hybrid film

During the past decade, 2D nanostructured materials have attracted intense research activity because of their unique physicochemical properties, such as an extremely high structural anisotropy and a high tendency to form stable colloidal suspensions.[1−4] One of the most effective methods for synthesizing 2D nanosheets is exfoliation, the separation of layered inorganic solids into individual layers through the intercalation of bulky organic molecules or interlayer evolution of H_2 gas.[5−8] To date, many kinds of layered inorganic solids such as clay minerals,[9,10] graphites,[11−13] metal oxides,[1,14−22] metal hydroxides,[23−25] metal chalcogenides,[26−28] and metal phosphates[29−32] have been exfoliated into individual 2D nanosheets. Since most of the colloidal nanosheets obtained by the exfoliation route possess a considerable amount of surface charge, these nanomaterials are used as building blocks for heterostructured nanohybrids and hierarchically assembled multilayered films.[33−38] Also, the lack of lattice energy stabilization along the *c*-axis makes this type of nanostructured material somewhat unstable, which means exfoliated nanosheets can be easily transformed into 1D nanowires/nanotubes or 0D hollow spheres under ambient or hydrothermal conditions.[39−42] Exfoliated nanosheets show a broad spectrum of physicochemical properties from insulating to metallic, and these properties can be tailored by changing the chemical formula of the pristine compound.[4,17,22,24,43]

Recently layered transition metal oxides are of prime importance as electrode materials for lithium ion batteries as well as for supercapacitors.[21,44,45] In terms of energy density and working potential, oxides of cobalt, nickel, and manganese are promising candidates for cathodes for Li^+ ion cell. Among them, layered $LiCoO_2$ has been successfully commercialized and adopted for most of lithium secondary batteries in current market.[44−46] However, because of the high price and high toxicity of cobalt ions, there have been increasing demands for the development of new economic cathode materials with better performance. The layered $Li[Mn_{1/3}Co_{1/3}Ni_{1/3}]O_2$ is attracting tremendous research interest as an alternative to cathode material because it has a larger capacity, higher thermal stability, and lower cobalt content than the current commercialized $LiCoO_2$.[47−49] Considering the layered structure of $Li[Mn_{1/3}Co_{1/3}Ni_{1/3}]O_2$ having exchangeable lithium ions in the interlayer space, exfoliation is expected to be applicable to this electrode material.

*Address correspondence to hwangsju@ewha.ac.kr.

Received for review February 11, 2010 and accepted July 02, 2010.

Published online July 13, 2010.
10.1021/nn100286u

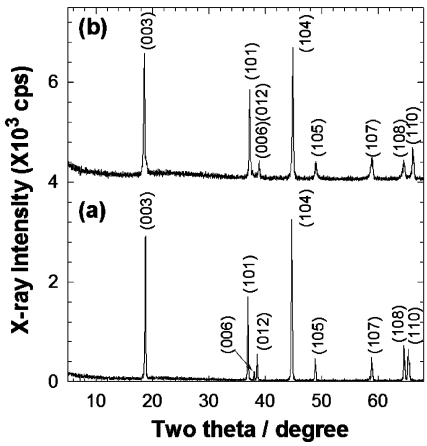

Figure 1. Powder XRD patterns of (a) the pristine $Li[Mn_{1/3}Co_{1/3}Ni_{1/3}]O_2$ and (b) the protonated derivative.

Exfoliated nanosheets of $Li[Mn_{1/3}Co_{1/3}Ni_{1/3}]O_2$ would allow us not only to optimize the electrochemical activity of this material but also to widen its application through hybridization with carbon nanotubes, graphene, and inorganic nanoclusters. In one instance, the hybridization of $[Mn_{1/3}Co_{1/3}Ni_{1/3}]O_2$ nanosheets with highly conducting material would be quite effective improving the electrode functionality of this layered metal oxide through the improvement of electrical conductivity. There is a great deal of research regarding $Li[Mn_{1/3}Co_{1/3}Ni_{1/3}]O_2$,[47,48] but at the time of the publication of the present study, we are aware of no other reports on the exfoliation of this metal oxide into individual monolayers.

Here we report the preparation of the exfoliated nanosheets of $[Mn_{1/3}Co_{1/3}Ni_{1/3}]O_2$ by the intercalation of quaternary ammonium cations into the layered $Li[Mn_{1/3}Co_{1/3}Ni_{1/3}]O_2$ lattice. Also, we have synthesized the layer-by-layer, or LBL, films comprising the obtained nanosheets and polycations.

RESULTS AND DISCUSSION

Powder XRD and TG-DTA Analyses for Protonated Metal Oxide. The effect of proton-exchange on the crystal structure of pristine $Li[Mn_{1/3}Co_{1/3}Ni_{1/3}]O_2$ was examined with powder X-ray diffraction, or XRD. As plotted in Figure 1, an acid-treatment for the pristine $Li[Mn_{1/3}Co_{1/3}Ni_{1/3}]O_2$ gave rise to a slight increase of basal spacing (Δc = 0.39 Å), which is interpreted as a result of the increase of electrostatic repulsion between $[Mn_{1/3}Co_{1/3}Ni_{1/3}]O_2$ layers.[50−52] In contrast to layered $K_{0.45}MnO_2$[17] and $Cs_{0.67}Ti_{1.83}\square_{0.17}O_4$,[14] no water could be intercalated into the layered manganese cobalt nickel oxide lattice with higher layer charge. Evolutions of the content of lithium and transition metal ions in the pristine compound upon the acid-treatment were examined using atomic emission spectroscopy-inductively coupled plasma spectrometry, or AES-ICP. We found that 3 days of treatment could remove 80% of interlayer lithium ions from $Li[Mn_{1/3}Co_{1/3}Ni_{1/3}]O_2$, but extending the treatment to 10 days could not induce further significant decrease in Li content (*i.e.*, 81% over 7 days and 82% over 10 days). In contrast to a marked decrease of lithium content by acid-treatment, there is no marked change in the ratio of Mn:Co:Ni (1/3:1/3:1/3), indicating negligible preferential dissolution of component metal ions.

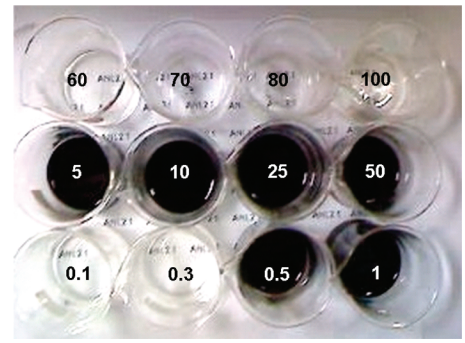

Figure 2. Photographs of supernant solution obtained from the reaction between the protonated $Li[Mn_{1/3}Co_{1/3}Ni_{1/3}]O_2$ and TMA · OH with the TMA^+/H^+ ratios of 0.1−100.

Also, we have estimated the contents of proton and water in the protonated derivative using iodometric titration and thermogravimetry-differential thermal analysis, or TG-DTA (see Supporting Information). TG-DTA analysis revealed that the acid-treated sample showed considerable weight loss in several temperature regions. First, there is a slight endothermic weight decrease in the temperature range of 100−200 °C, which corresponds to the removal of surface adsorbed water ($0.056H_2O$ per unit formula). The more prominent endothermic weight loss in the higher temperature region of 200−500 °C is attributable to dehydroxylation or dehydration linked to the deprotonation process. The oxygen loss from high-valent manganese cobalt nickel oxide is responsible for the endothermic weight decrease occurring beyond 600 °C.[53] From the iodometric titration, the average oxidation state of transition metal ions was determined as 3.29 ± 0.05.[54] On the basis of the results of AES-ICP, iodometric titration, and TG-DTA, the chemical formula of the protonated derivative was determined as $Li_{0.18}H_{0.53}[Mn_{1/3}Co_{1/3}Ni_{1/3}]O_2 \cdot 0.056H_2O$.

Exfoliation Behavior of Layered Manganese Cobalt Nickel Oxide. Exfoliation of the $Li[Mn_{1/3}Co_{1/3}Ni_{1/3}]O_2$ was achieved by reacting the protonated derivative with tetramethylammonium hydroxide, or TMA · OH, for 14 days. Following the reaction, the protonated $Li[Mn_{1/3}Co_{1/3}Ni_{1/3}]O_2$ crystallites were exfoliated, leading to the formation of a dark brown colloidal suspension. The exfoliation behavior of the protonated compound at various TMA^+/H^+ ratios was investigated by varying the concentration of aqueous TMA solution against the proton content in the protonated compound. We found that there is a strong dependency of the exfoliation behavior of the layered manganese cobalt nickel oxide on TMA concentration. As illustrated in Figure 2, exfoliation

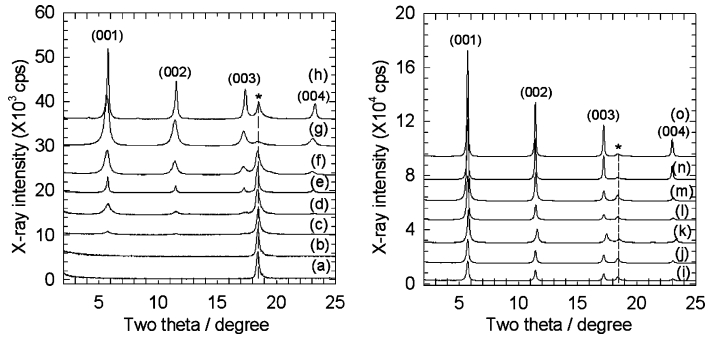

Figure 3. Powder XRD patterns of solid precipitates obtained from the reaction between the protonated $Li[Mn_{1/3}Co_{1/3}Ni_{1/3}]O_2$ and TMA · OH with various TMA^+/H^+ ratios: (a) 0.1, (b) 0.3, (c) 0.5, (d) 0.8, (e) 1, (f) 2, (g) 3, (h) 4, (i) 5, (j) 10, (k) 50, (l) 60, (m) 70, (n) 80, and (o) 100. The asterisks denote the (001) peak of the protonated phase.

occurred when the TMA^+/H^+ ratio was 0.5−50. Reactions outside this range produced no colloidal suspension, but all the manganese cobalt nickel oxides precipitated.

We separated a small amount of precipitate at the bottom of the as-prepared suspension by centrifugation at 6000 rpm (relative centrifugal force, 9009*G*) for 15 min, resulting in a pure colloidal suspension.

The crystal structures of the obtained precipitates were examined with powder XRD. As shown in Figure 3, reactions with a TMA^+/H^+ ratio of 0.1−0.3 gave precipitates of protonated metal oxide with a basal spacing of $d_{001} = 4.92$ Å, whereas the reactions with a TMA^+/H^+ ratio ≥0.5 led to the synthesis of organic intercalate with expanded basal spacings ($d_{001} = 15.68$ Å) as well as the protonated metal oxide. As the concentration of TMA^+ ions increased, the XRD peaks of the organic intercalate grew stronger whereas those of the protonated phase became depressed. The enhancement of peak intensity and peak sharpness suggests an improvement in the layer-by-layer ordering of the intercalation phase. Similar evolution of XRD patterns upon the change of guest ammonium concentration was reported for layered manganese oxide or layered titanium oxide.[6,14,17,22] According to the previous literatures about the exfoliation of layered metal oxides,[14,17] the formation of individually exfoliated nanosheets can be achieved *via* intercalation, exfoliation, and osmotic swelling processes. T. Sasaki *et al.* reported that the swelling and exfoliation behaviors of layered metal oxides are sensitively dependent on the concentration of bulky organic ammonium cations against proton in the host lattice.[14,17] That is, an exfoliation into single sheets was promoted at lower ammonium content, whereas osmotic swelling was predominant at higher ammonium content. As a consequence, a well-ordered intercalation phase (*i.e.*, short-range swollen phase) is reconstructed from the exfoliated sheets by increasing the concentration of organic cation, as seen in the present results. As illustrated in Figure 3, a well-ordered swollen phase with expanded basal spacing ($d_{001} = 15.68$ Å) could be obtained in the TMA^+/H^+ range of 0.5−50, together with the colloidal suspension of exfoliated nanosheets. This indicates that the intercalation, osmotic swelling, and exfoliation processes of layered $[Mn_{1/3}Co_{1/3}Ni_{1/3}]O_2$ take place simultaneously. In the case of $TMA^+/H^+ > 50$, only a well-ordered swollen phase could be prepared, underscoring that reconstruction of the intercalation structure from exfoliated nanosheets is more predominant at high guest concentration, as reported for other layered metal oxides.[14,17] The predominant swelling of layered metal oxide at higher guest concentration is interpreted as a result of an enhanced attraction between guest ammonium cations and negatively charged exfoliated metal oxide nanosheets. Also, we carried out AES-ICP analyses for the protonated sample reacted with TMA^+ to probe variations in the content of Li ions caused by the intercalation of TMA^+ ions. The highly swollen phase obtained with the TMA^+/H^+ ratio of 60 shows a Li/(Mn + Co + Ni) ratio of ~0.2, which is nearly the same as that of the protonated derivative. This finding underscores that the guest TMA^+ ions replace the protons in the protonated metal oxide, not the lithium ions. Thus, the concentration of lithium ions in the protonated derivative remains nearly unchanged after the reaction with TMA^+ ions.

Characterization of Exfoliated Manganese Cobalt Nickel Oxide Nanosheets. We have carried out systematic characterization on the pure colloidal suspension obtained by the above-mentioned centrifugation process. As shown in the left panel of Figure 4a, the observation of the Tyndall phenomenon with the pure colloidal suspension, characteristic of exfoliated colloids, provides strong evidence for the exfoliation of $Li[Mn_{1/3}Co_{1/3}Ni_{1/3}]O_2$. The exfoliated nanosheets were restored from pure colloidal suspension by high-speed centrifugation at 17000 rpm (relative centrifugal force, 25525*G*) for >30 min. The powder XRD pattern of the restored sample in the wet state was plotted in the right panel of Figure 4a, showing a long tail in low angle of $2\theta < 10°$. This reflects the disordered filing of exfoliated nanosheets characteristic of the previously reported nanosheets of other binary metal oxides.[14,17,55−57] A very similar XRD feature has been reported for the colloidal nanosheets of layered titanate, layered

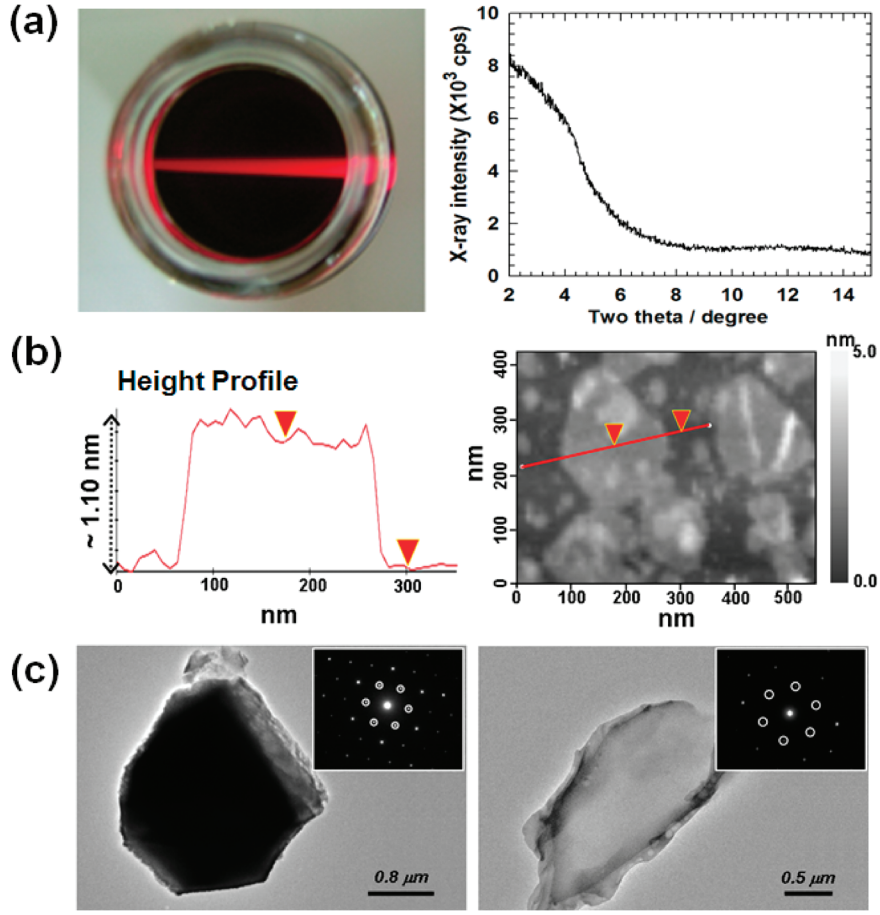

Figure 4. (a) Photograph (left) and XRD pattern (right) of exfoliated $[Mn_{1/3}Co_{1/3}Ni_{1/3}]O_2$ nanosheets. (b) Height profile (left) and AFM image (right) of the exfoliated $[Mn_{1/3}Co_{1/3}Ni_{1/3}]O_2$ nanosheets adsorbed onto mica substrate. (c) HR-TEM/SAED data of (left) the protonated $Li[Mn_{1/3}Co_{1/3}Ni_{1/3}]O_2$ and (right) exfoliated nanosheets.

manganate, and others.[14,17,57] As with other layered metal oxides, exfoliation is believed to occur by the solvation of TMA^+ and $[Mn_{1/3}Co_{1/3}Ni_{1/3}]O_2$ layer.[14,17,55−57] The formation of the nanometer-thick monolayers by exfoliation is further confirmed by the atomic force microscopy, or AFM, image of Figure 4b. Nanosheet thickness was calculated from the height of the nanosheets with respect to the substrate surface.[17,56] The unilamellar $[Mn_{1/3}Co_{1/3}Ni_{1/3}]O_2$ nanosheets clearly show the plate-type morphology, with lateral dimensions of hundreds of nanometers and a thickness of $\sim 1.10 \pm 0.1$ nm. The thickness of the oxide nanosheet observed by AFM is, however, somewhat different from that estimated from crystallographic information of individual layers.[58,59] Considering the adsorption of TMA^+ molecules with a theoretical size of 0.50−0.60 nm and/or the hydration layers on the surface of oxide nanosheets,[58,60] we regarded the measured thickness as clear evidence of the formation of unilamellar $[Mn_{1/3}Co_{1/3}Ni_{1/3}]O_2$ nanosheets. Such a degree of thickness discrepancy in the AFM data was commonly observed for most of the reported inorganic nanosheets.[17,61]

According to high resolution-transmission electron microscopy, or HR-TEM, the protonated and exfoliated $[Mn_{1/3}Co_{1/3}Ni_{1/3}]O_2$ commonly show the images of a plate-shaped crystallite (Figure 4c). But the much weaker contrast of the exfoliated form compared with the protonated form is indirect evidence of exfoliation into very thin $[Mn_{1/3}Co_{1/3}Ni_{1/3}]O_2$ nanosheets. Although the very weak intensity of the in-plane (*hk*0) peaks in the XRD data of the restored sample prevents us from detecting these peaks with a conventional XRD instrument (Figure 4a),[17] the observation of hexagonal diffraction spots in the selected area electron diffraction, or SAED, patterns of the exfoliated nanosheets underscores the maintenance of the hexagonal lattice of the layered manganese cobalt nickel oxide upon exfoliation, as presented in Figure 4c. To confirm the maintenance of hexagonal layered structure of this material after the exfoliation, we tried to reassemble the colloidal nanosheets of $[Mn_{1/3}Co_{1/3}Ni_{1/3}]O_2$ with Li^+ ions. The crystal structure of the obtained reassembled material was examined with powder XRD analysis (see Supporting Information). In addition to the (001) XRD peaks reflecting the formation of the hydrated intercalation phase of the layered metal oxide, the reassembled

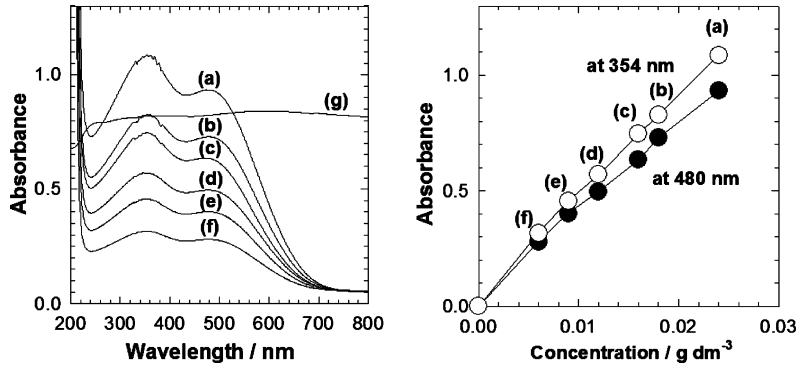

Figure 5. (Left) UV−vis spectra and (right) absorbance at 354 and 480 nm for the colloidal suspensions at concentrations of (a) 2.4 × 10^{-2}, (b) 1.80 × 10^{-2}, (c) 1.60 × 10^{-2}, (d) 1.20 × 10^{-2}, (e) 0.90 × 10^{-2}, (f) 0.60 × 10^{-2} g dm^{-3}, and (g) the protonated $Li[Mn_{1/3}Co_{1/3}Ni_{1/3}]O_2$.

sample shows distinct in-plane reflections of (10) and (11) at $2\theta = 36.5°$ and 65.6°, respectively. The restoration of these in-plane peaks after the reassembling of the exfoliated nanosheets provided strong evidence for the preservation of the hexagonal atomic arrangement of the $[Mn_{1/3}Co_{1/3}Ni_{1/3}]O_2$ nanosheets. Elemental analysis clearly demonstrates negligible change in the relative contents of Mn, Co, and Ni after exfoliation.

We have probed the optical property of the colloidal suspension of exfoliated manganese cobalt nickel oxide using ultraviolet−visible, or UV−vis spectroscopy. In Figure 5, the UV−vis spectra of the pure colloidal suspension of $[Mn_{1/3}Co_{1/3}Ni_{1/3}]O_2$ nanosheets display two distinct absorption peaks. We attribute the peak at ~354 nm to the overlap of the d−d transitions of manganese and nickel ions in the octahedral site, whereas the other peak, at ~480 nm, corresponds to that of octahedral cobalt ions.[17,62−64] The distinct absorption peaks contrast with the featureless spectrum of the protonated $Li[Mn_{1/3}Co_{1/3}Ni_{1/3}]O_2$. Since the protonated metal oxide possesses metallic band structure without the opening of bandgap, this material can absorb all the wavelength region of ultraviolet and visible light, leading to the featureless UV−vis spectrum. Hence, the appearance of the distinct absorption peaks after the exfoliation provides strong evidence for the transformation of metallic solids into molecule-like nanosheets. Such a remarkable change in the optical property of pristine material upon the exfoliation was already reported for other layered metal oxides like layered manganese oxide.[17,22] The absorbance at 354 and 480 nm is linearly proportional to the concentration of colloidal particles, strongly suggesting no agglomeration of exfoliated nanosheets in the given concentration range.[14,17] From the present UV−vis results, the respective molar absorption coefficients at 354 and 480 nm were determined as 4.05 × 10^3 and 3.48 × 10^3 mol^{-1} dm^3 cm^{-1}.

LBL Deposition of Heterolayer Film with Polycations. We have studied the surface charges of manganese cobalt nickel oxide colloidal particles with zeta potential measurement (see Supporting Information). Zeta potential measurements indicated that $[Mn_{1/3}Co_{1/3}Ni_{1/3}]O_2$ nanosheets have a negative surface charge with the potential of −68 mV. In light of this data, we fabricated poly(diallyldimethlammonium)-conjugated, or PDDA-conjugated, hybrid film through successive LBL coatings of the colloidal nanosheets and PDDA.

We have probed the stacking structure of the coated films using powder XRD analysis. As shown in the left panel of Figure 6, the coated films with a larger number of multilayers showed a distinct (001) reflection at low angle side, indicating the layer-by-layer ordered stacking of manganese cobalt nickel oxide crystallites and PDDA polymers. The observed XRD feature is quite similar to that of the previously reported MnO_2/PDDA heterolayered film.[65] As the number of layers increased, the color of the glass substrate changed to a dark-

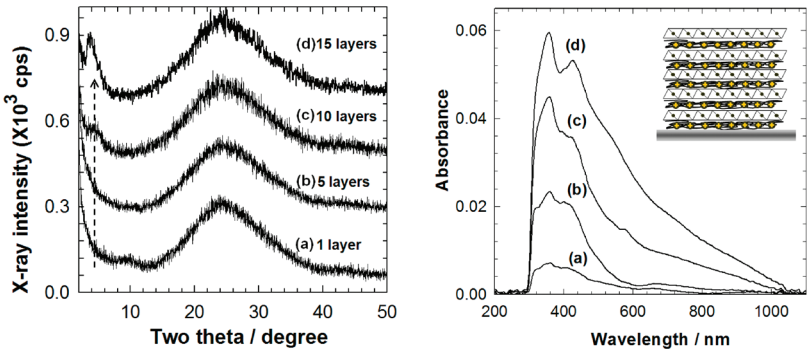

Figure 6. (Left) Powder XRD patterns and (right) UV−vis spectra/schematic model of the conjugated films of $[Mn_{1/3}Co_{1/3}Ni_{1/3}]O_2$−PDDA with (a) 1, (b) 5, (c) 10, and (d) 15 layers.

brown, the color of colloidal suspension (see Supporting Information). As shown in the UV−vis spectra of the right panel of Figure 6, the obtained hybrid film exhibits the characteristic absorption peaks of a colloidal suspension, which contrasts sharply with the featureless spectrum of the protonated $Li[Mn_{1/3}Co_{1/3}Ni_{1/3}]O_2$. Even with slight peak shifts because of the interaction with polycations, the observation of distinct absorption peaks for the hybrid film makes it clear that the unilamellar nanosheets are intact after interstratification with PDDA.

As described in the introduction section, the exfoliated nanosheets can be used as useful building blocks for novel superstructured or composited materials with expanded surface area such as organic−inorganic nanocomposites, hollow sphere, porous assembly, etc.[66−72] We expected that these novel materials synthesized with exfoliated nanosheets can be used as effective electrode materials for supercapacitors or Li^+-ion secondary batteries.[69−72] On the basis of this expectation, we tried to hybridize $[Mn_{1/3}Co_{1/3}Ni_{1/3}]O_2$ nanosheets with polyaniline (PANI) *via* the *in situ* polymerization of aniline in the colloidal suspension of $[Mn_{1/3}Co_{1/3}Ni_{1/3}]O_2$. The preliminary electrochemistry test clearly demonstrated that the obtained PANI-$[Mn_{1/3}Co_{1/3}Ni_{1/3}]O_2$ nanocomposite shows much larger capacitance by more than five times than the pristine metal oxide. This result clearly demonstrated the usefulness of exfoliated nanosheets in developing new efficient electrode materials applicable for supercapacitor.

CONCLUSION

We successfully prepared unilamellar nanosheets of layered $[Mn_{1/3}Co_{1/3}Ni_{1/3}]O_2$ and synthesized its polymer-conjugated LBL film. The exfoliation of layered manganese cobalt nickel oxide into individual $[Mn_{1/3}Co_{1/3}Ni_{1/3}]O_2$ monolayers with a thickness of <1 nm was confirmed with AFM, HR-TEM, and UV−vis. The results of our SAED analyses clearly demonstrated that the hexagonal in-plane structure of the layered manganese cobalt nickel oxide is well maintained before and after the protonation and exfoliation processes. Also, we fabricated heterolayered films of manganese cobalt nickel oxide and PDDA through a successive coating of colloidal suspension and polycations. The present multicomponent metal oxide nanosheets are potentially very useful as building blocks for hierarchically assembled superstructures and films of lithium intercalation electrodes.

METHODS

Preparation. The pristine $Li[Mn_{1/3}Co_{1/3}Ni_{1/3}]O_2$ compound was synthesized by the following procedure: first the precursor $[Mn_{1/3}Co_{1/3}Ni_{1/3}]O_2$ was prepared by the sol−gel method using citric acid as a polymeric agent. That is, a stoichiometric amount of Mn, Co, and Ni acetate salts (cationic molar ratio of Mn:Co:Ni = 1:1:1) were dissolved in an aqueous solution of citric acid. The obtained solution was slowly heated up to 80 °C to evaporate water. During heat-treatment, the solution pH was maintained to ~6. The resulting power was sintered at 400 °C, leading to the preparation of the precursor $[Mn_{1/3}Co_{1/3}Ni_{1/3}]O_2$ powder. Finally the obtained precursor powder was mixed with Li_2CO_3 and then sintered at 900 °C, leading to the synthesis of single phase $Li[Mn_{1/3}Co_{1/3}Ni_{1/3}]O_2$ material. Proton exchange for the pristine compound was done by the reaction between the $Li[Mn_{1/3}Co_{1/3}Ni_{1/3}]O_2$ sample (1 g) and 1 M aqueous HCl solution (100 cm^3) at room temperature. During the proton exchange reaction, the HCl solution was replaced with a fresh one everyday. The exfoliation of this metal oxide was achieved by reacting the protonated material (0.5 g) with 100 cm^3 of an aqueous tetramethylammonium hydroxide (TMA · OH) solution for more than 2 weeks. To investigate the effect of TMA^+ concentration on exfoliation efficiency, we have carried out the reactions between TMA^+ and the protonated metal oxide with various TMA^+/H^+ ratio of 0.1−100.

Fabrication of LBL Hybrid Films. For the fabrication of LBL hybrid film composed of $[Mn_{1/3}Co_{1/3}Ni_{1/3}]O_2$ nanosheets and polycations, the quartz slide glass was used as solid substrate. Prior to the film deposition, the substrate was washed according to the procedure reported previously.[35] Then, the substrate was precoated by immersing it in an aqueous solution of polyethyleneimine (PEI, 2.5 g cm^{-3}) at pH ≈ 9.0 for 20 min to create the positively charged surface of substrate. After being washed with distilled water, the PEI-primed substrate was dipped into the colloidal suspension of exfoliated nanosheets (0.05 g dm^{-3}) for 20 min, followed by washing with distilled water. Then, the PEI/nanosheets-coated substrate was dipped into aqueous solution of polydiallyldimethylammonium (PDDA, 2.5 g cm^{-3}) for 20 min, followed by washing with distilled water. This stepwise coating process with exfoliated nanosheets and PDDA was repeatedly conducted. After the completion of successive coating, the obtained multilayer hybrid film was washed with distilled water and dried.

Characterization. The chemical compositions of the present samples were determined using AES-ICP (PerkinElmer, Optima-4300 DV). The thermal behavior of the protonated manganese cobalt nickel oxide was examined with TG-DTA (PerkinElmer, Pyris) under nitrogen atmosphere at the rate of 5 °C/min. To determine the average oxidation state of component metal ions in the samples, we have carried out the iodometric redox titration, as reported by previous literature.[54] Typically, an accurately weighed sample (*ca.* 35 mg) of the protonated manganese cobalt nickel oxide was dissolved in mixed solution of 6 M HCl (*ca.* 100 mL) and excess KI (*ca.* 3 g). Generated neutral iodine (I_2) in the solution was titrated with standardized sodium thiosulfate ($Na_2S_2O_3$) solution (*ca.* 0.012 M). The crystal structures of the present materials were studied by powder XRD measurement using a Rigaku diffractometer with Ni-filtered Cu Kα radiation (λ = 1.5418 Å) and a graphite diffracted beam monochromator. We used UV−vis spectroscopy to study the optical property of the colloidal suspensions. UV−vis spectra were measured with a Perkin-Elmer Lambda 35 spectrometer. For a solid sample, the diffuse reflectance UV−vis spectrum was obtained with an integrating sphere, using $BaSO_4$ as a reference. The crystallite shape and crystal structure of the protonated $Li[Mn_{1/3}Co_{1/3}Ni_{1/3}]O_2$ and its exfoliated nanosheets were probed by performing HR-TEM/SAED measurements with a Jeol JEM-2100F microscope at an accelerating voltage of 200 kV. We probed the thickness and crystallite dimension of the exfoliated $[Mn_{1/3}Co_{1/3}Ni_{1/3}]O_2$ nanosheets by using AFM (PSIA, XE-100). For AFM analysis, the exfoliated nanosheets were adsorbed onto a mica substrate coated with PEI, as reported previously.[17] A zeta potential of the colloidal suspension of the exfoliated $[Mn_{1/3}Co_{1/3}Ni_{1/3}]O_2$ nanosheets was measured with the Zetasizer Nano ZS (Malvern Instruments).

The diluted colloidal suspension was kept at 25 °C and started to circulate into the zeta cell. After stabilization for 35 min, the zeta potential of the exfoliated $[Mn_{1/3}Co_{1/3}Ni_{1/3}]O_2$ nanosheets was measured.

Acknowledgment. This research was supported by the Converging Research Center Program through the National Research Foundation of Korea (NRF) funded by the Ministry of Education, Science and Technology (20090093646), by the Korea Research Foundation Grant funded by the Korean Government (KRF-2008-313-C00442), and partly by the National Research Foundation of Korea Grant funded by the Korean Government (2010-0001485). The experiments at PAL were supported in part by MOST and POSTECH.

Supporting Information Available: The TG-DTA curve of the protonated derivative, the zeta potential data of the colloidal suspension, the power XRD pattern of reassembled Li^+-$[Mn_{1/3}Co_{1/3}Ni_{1/3}]O_2$ sample, and the photoimage of the conjugated films of $[Mn_{1/3}Co_{1/3}Ni_{1/3}]O_2$−PDDA. These materials are available free of charge *via* the Internet at http://pubs.acs.org.

REFERENCES AND NOTES

1. Treacy, M. M. J.; Rice, S. B.; Jacobson, A. J.; Lewandowski, J. T. Electron Microscopy Study of Delamination in Dispersions of the Perovskite-Related Layered Phases $K[Ca_2Na_{n-3}Nb_nO_{3n-1}]$: Evidence for Single-Layer Formation. *Chem. Mater.* **1990**, *2*, 279–286.
2. Jacobson, A. J. In *Comprehensive Supramolecular Chemistry*; Alberti, G., Bein, T., Eds.; Elsevier: Oxford, UK, 1996; Vol. 7, pp 315−335.
3. Moriarty, P. Nanostructured Materials. *Rep. Prog. Phys.* **2001**, *64*, 297–381.
4. Auerbach, S. M., Carrado, K. A.; Dutta, P. K., Eds. *Handbook of Layered Materials*; Marcel Dekker: New York, 2004.
5. Kim, J. -Y.; Chung, I.; Choy, J. -H.; Park, G. -S. Macromolecular Nanoplatelet of Aurivillius-Type Layered Perovskite Oxide, $Bi_4Ti_3O_{12}$. *Chem. Mater.* **2001**, *13*, 2759–2761.
6. Liu, Z. -H.; Ooi, K.; Kanoh, H.; Tang, W. -P.; Tomida, T. Swelling and Delamination Behaviors of Birnessite-Type Manganese Oxide by Intercalation of Tetraalkylammonium Ions. *Langmuir* **2000**, *16*, 4154–4164.
7. Gao, Q.; Giraldo, O.; Tong, W.; Suib, S. L. Preparation of Nanometer-Sized Manganese Oxides by Intercalation of Organic Ammonium Ions in Synthetic Birnessite OL-1. *Chem. Mater.* **2001**, *13*, 778–786.
8. Tsunoda, Y.; Sugimoto, W.; Sugahara, Y. Intercalation Behavior of *n*-Alkylamines into a Protonated Form of a Layered Perovskite Derived from Aurivillius Phase $Bi_2SrTa_2O_9$. *Chem. Mater.* **2003**, *15*, 632–635.
9. Walker, G. F. Macroscopic Swelling of Vermiculite Crystals in Water. *Nature* **1960**, *187*, 312–313.
10. Nadeau, P. H.; Wilson, M. J.; McHardy, W. J.; Tait, J. M. Interstratified Clays as Fundamental Particles. *Science* **1984**, *225*, 923–925.
11. Liu, P.; Gong, K. Synthesis of Polyaniline-Intercalated Graphite Oxide by an *in Situ* Oxidative Polymerization Reaction. *Carbon* **1999**, *37*, 706–707.
12. Liu, Z. -H.; Wang, Z. -M.; Yang, X.; Ooi, K. Intercalation of Organic Ammonium Ions into Layered Graphite Oxide. *Langmuir* **2002**, *18*, 4926–4932.
13. Li, X.; Zhang, G.; Bai, X.; Sun, X.; Wang, X.; Wang, E.; Dai, H. Highly Conducting Graphene Sheets and Langmuir-Blodgett Films. *Nat. Nanotechnol.* **2008**, *3*, 538–542.
14. Sasaki, T.; Watanabe, M. Osmotic Swelling to Exfoliation. Exceptionally High Degrees of Hydration of a Layered Titanate. *J. Am. Chem. Soc.* **1998**, *120*, 4682–4689.
15. Miyamoto, N.; Kuroda, K.; Ogawa, M. Exfoliation and Film Preparation of a Layered Titanate, $Na_2Ti_3O_7$, and Intercalation of Pseudoisocyanine Dye. *J. Mater. Chem.* **2004**, *14*, 165–170.
16. Fukuda, K.; Akatsuka, K.; Ebina, Y.; Ma, R.; Takada, K.; Nakai, I.; Sasaki, T. Exfoliated Nanosheet Crystallite of Cesium Tungstate with 2D Pyrochlore Structure: Synthesis, Characterization, and Photochromic Properties. *ACS Nano* **2008**, *2*, 1689–1695.
17. Omomo, Y.; Sasaki, T.; Wang, L. Z.; Watanabe, M. Redoxable Nanosheet Crystallites of MnO_2 Derived *via* Delamination of a Layered Manganese Oxide. *J. Am. Chem. Soc.* **2003**, *125*, 3568–3575.
18. Schaak, R. E.; Mallouk, T. E. Perovskites by Design: A Toolbox of Solid-State Reactions. *Chem. Mater.* **2002**, *14*, 1455–1471.
19. Shaak, R. E.; Mallouk, T. E. Exfoliation of Layered Rutile and Perovskite Tungstates. *Chem. Commun.* **2002**, 706–707.
20. Takagaki, A.; Lu, D.; Kondo, J. N.; Hara, M.; Hayashi, S.; Domen, K. Exfoliated HNb_3O_8 Nanosheets as a Strong Protonic Solid Acid. *Chem. Mater.* **2005**, *17*, 2487–2489.
21. Sugimoto, W.; Iwata, H.; Yasunaga, Y.; Murakami, Y.; Takasu, Y. Preparation of Ruthenic Acid Nanosheets and Utilization of Its Interlayer Surface for Electrochemical Energy Storage. *Angew. Chem.* **2003**, *42*, 4092–4096.
22. Kim, T. W.; Oh, E. J.; Lim, S. T.; Park, D. H.; Jee, A. Y.; Lee, M.; Hyun, S. -H.; Choy, J. -H.; Hwang, S. -J. Exfoliated Nanosheets of Layered Cobalt Oxide and Their Application for Film Deposition and Nanoparticle Synthesis. *Chem.—Eur. J.* **2009**, *15*, 10752–10761.
23. Adachi-Pagano, M.; Forano, C.; Besse, J. Delamination of Layered Double Hydroxides by Use of Surfactants. *Chem. Commun.* **2000**, 91–92.
24. Hibino, T.; Jones, W. New Approach to the Delamination of Layered Double Hydroxides. *J. Mater. Chem.* **2001**, *11*, 1321–1323.
25. Li, L.; Ma, R.; Ebina, Y.; Iyi, N.; Sasaki, T. Positively Charged Nanosheets Derived *via* Total Delamination of Layered Double Hydroxides. *Chem. Mater.* **2005**, *17*, 4386–4391.
26. Leaf, A.; Schöllhorn, R. Solvation Reactions of Layered Ternary Sulfides A_xTiS_2, A_xNbS_2, and A_xTaS_2. *Inorg. Chem.* **1977**, *16*, 2950–2956.
27. Joensen, P.; Frindt, R. F.; Morrison, S. R. Single-Layer MoS_2. *Mater. Res. Bull.* **1986**, *21*, 457–461.
28. Yang, D.; Frindt, R. F. Li-Intercalation and Exfoliation of WS_2. *J. Phys. Chem. Solids* **1996**, *57*, 1113–1116.
29. Tindwa, R. M.; Ellis, D. K.; Peng, G. Z.; Clearfield, A. Intercalation of *n*-Alkylamines by α-Zirconium Phosphate. *J. Chem. Soc., Faraday Trans.* **1985**, *81*, 545–552.
30. Kim, H. N.; Keller, S. W.; Mallouk, T. E. Characterization of Zirconium Phosphate/Polycation Thin Films Grown by Sequential Adsorption Reactions. *Chem. Mater.* **1997**, *9*, 1414–1421.
31. Alberti, G.; Dionigi, C.; Giontella, E.; Murcia-Mascaros, S. Formation of Colloidal Dispersions of Layered γ-Zirconium Phosphate in Water/Acetone Mixtures. *J. Colloid Interface Sci.* **1997**, *188*, 27–31.
32. Alberti, G.; Giontella, E.; Murcia-Mascarós, S. Mechanism of the Formation of Organic Derivatives of γ-Zirconium Phosphate by Topotactic Reactions with Phosphonic Acids in Water and Water−Acetone Media. *Inorg. Chem.* **1997**, *36*, 2844–2849.
33. Paek, S. -M.; Jung, H.; Lee, Y. -J.; Park, M.; Hwang, S. -J.; Choy, J. -H. Exfoliation and Reassembling Route to Mesoporous Titania Nanohybrids. *Chem. Mater.* **2006**, *18*, 1134–1140.
34. Hur, S. G.; Kim, T. W.; Hwang, S. -J.; Hwang, S. -H.; Yang, J. H.; Choy, J. -H. Heterostructured Nanohybrid of Zinc Oxide−Montmorillonite Clay. *J. Phys. Chem. B* **2006**, *110*, 1599–1604.
35. Sasaki, T.; Ebina, Y.; Fukuda, K.; Tanaka, T.; Harada, M.; Watanabe, M. Titania Nanostructured Films Derived from a Titania Nanosheet/Polycation Multilayer Assembly *via* Heat Treatment and UV Irradiation. *Chem. Mater.* **2002**, *14*, 3524–3530.
36. Yang, X.; Makita, Y.; Liu, Z. -H.; Ooi, K. Novel Synthesis of Layered Graphite Oxide-Birnessite Manganese Oxide Nanocomposite. *Chem. Mater.* **2003**, *15*, 1228–1231.
37. Wang, L.; Sakai, N.; Ebina, Y.; Takada, K.; Sasaki, T. Inorganic Multilayer Films of Manganese Oxide Nanosheets and Aluminum Polyoxocations: Fabrication, Structure, and

Electrochemical Behavior. *Chem. Mater.* **2005**, *17*, 1352–1357.
38. Li, L.; Ebina, Y.; Fukuda, K.; Takada, K.; Sasaki, T. Layer-by-Layer Assembly and Spontaneous Flocculation of Oppositely Charged Oxide and Hydroxide Nanosheets into Inorganic Sandwich Layered Materials. *J. Am. Chem. Soc.* **2007**, *129*, 8000–8007.
39. Saupe, G. B.; Waraksa, C. C.; Kim, H. -N.; Han, Y. J.; Kaschak, D. M.; Skinner, D. M.; Mallouk, T. E. Nanoscale Tubules Formed by Exfoliation of Potassium Hexaniobate. *Chem. Mater.* **2000**, *12*, 1556–1562.
40. Wang, L.; Ebina, Y.; Takada, K.; Sasaki, T. Ultrathin Films and Hollow Shells with Pillared Architectures Fabricated *via* Layer-by-Layer Self-Assembly of Titania Nanosheets and Aluminum Keggin Ions. *J. Phys. Chem. B* **2004**, *108*, 4283–4288.
41. Schaak, R. E.; Mallouk, T. E. Prying Apart Ruddlesden-Popper Phases: Exfoliation into Sheets and Nanotubes for Assembly of Perovskite Thin Films. *Chem. Mater.* **2000**, *12*, 3427–3434.
42. Kobayashi, Y.; Hata, H.; Salama, M.; Mallouk, T. E. Scrolled Sheet Precursor Route to Niobium and Tantalum Oxide Nanotubes. *Nano Lett.* **2007**, *7*, 2142–2145.
43. Dong, X.; Osada, M.; Ueda, H.; Ebina, Y.; Kotani, Y.; Ono, K.; Ueda, S.; Kobayshi, K.; Takada, K.; Sasaki, T. Synthesis of Mn-Substituted Titania Nanosheets and Ferromagnetic Thin Films with Controlled Doping. *Chem. Mater.* **2009**, *21*, 4366–4373.
44. Whittingham, M. S. Lithium Batteries and Cathode Materials. *Chem. Rev.* **2004**, *10*, 4271–4302.
45. Tarascon, J. -M.; Armand, M. Issues and Challenges Facing Rechargeable Lithium Batteries. *Nature* **2001**, *414*, 359–367.
46. Mizushima, K.; Jones, P. C.; Wiseman, P. J.; Goodenough, J. B. Li_xCoO_2 ($0 < x \leq 1$): A New Cathode Material for Batteries of High Energy Density. *Mater. Res. Bull.* **1980**, *15*, 783–789.
47. Ohzuku, T.; Makimura, Y. Layered Lithium Insertion Material of $LiCo_{1/3}Ni_{1/3}Mn_{1/3}O_2$ for Lithium-Ion Batteries. *Chem. Lett.* **2001**, *30*, 642–643.
48. Yabuuchi, N.; Ohzuku, T. Novel Lithium Insertion Material of $LiCo_{1/3}Ni_{1/3}Mn_{1/3}O_2$ for Advanced Lithium-Ion Batteries. *J. Power Sources* **2003**, *119*, 171–174.
49. Lu, W.; Chen, Z.; Joachin, H.; Prakash, J.; Liu, J.; Amine, K. Electrochemical Characterization of MCMB/$LiNi_{1/3}Mn_{1/3}Co_{1/3}O_2$ Using LiBoB as an Electrolyte Additive. *J. Power Sources* **2007**, *163*, 1074–1079.
50. Ohzuku, T.; Ueda, A.; Nagayama, M. Electrochemistry and Structural Chemistry of $LiNiO_2$ ($R\bar{3}m$) for 4 V Secondary Lithium Cells. *J. Electrochem. Soc.* **1993**, *140*, 1862–1870.
51. Choi, J.; Manthiram, A. Role of Chemical and Structural Stabilities on the Electrochemical Properties of Layered $LiNi_{1/3}Mn_{1/3}Co_{1/3}O_2$ Cathodes. *J. Electrochem. Soc.* **2005**, *152*, A1714–A1718.
52. Idemoto, Y.; Matsui, T. Thermodynamic Stability, Crystal Structure, and Cathodic Performance of $Li_x(Mn_{1/3}Co_{1/3}Ni_{1/3})O_2$ Depend On the Synthetic Process and Li Content. *Solid State Ionics* **2008**, *179*, 625–635.
53. Ren, Z.; Wang, Y. -W.; Liu, S.; Wang, J.; Xu, Z. -A.; Cao, G. -H. Synthesis of Cobalt Oxyhydrate Superconductor through a Disproportionation Reaction Route. *Chem. Mater.* **2005**, *17*, 1501–1504.
54. Karppinen, M.; Matvejeff, M.; Salomaki, K.; Yamauchi, H. Oxygen Content Analysis of Functional Perovskite-Derived Cobalt Oxides. *J. Mater. Chem.* **2002**, *12*, 1761–1764.
55. Ma, R.; Takada, K.; Fukuda, K.; Iyi, N.; Bando, Y.; Sasaki, T. Topochemical Synthesis of Monometallic ($Co^{2+}-Co^{3+}$) Layered Double Hydroxide and Its Exfoliation into Positively Charged $Co(OH)_2$ Nanosheets. *Angew. Chem., Int. Ed.* **2008**, *47*, 86–89.
56. Ma, R.; Liu, Z.; Takada, K.; Iyi, N.; Bando, Y.; Sasaki, T. Synthesis and Exfoliation of $Co^{2+}-Fe^{3+}$ Layered Double Hydroxides: An Innovative Topochemical Approach. *J. Am. Chem. Soc.* **2007**, *129*, 5257–5263.
57. Hata, H.; Kubo, S.; Kobayashi, Y.; Mallouk, T. E. Intercalation of Well-Dispersed Gold Nanoparticles into Layered Oxide Nanosheets through Intercalation of a Polyamine. *J. Am. Chem. Soc.* **2007**, *129*, 3064–3065.
58. The theoretical monolayer thickness (~0.56 nm) of cobalt nickel manganese oxide layer is estimated from ionic radius in Shannon, R. D. *Acta Crystallogr.* **1976**, *A32*, 751–767.
59. We calculated the crystallographic thickness of $[Mn_{1/3}Co_{1/3}Ni_{1/3}]O_2$ nanosheet using ionic radius of component ions (Shannon, R. D. *Acta Crystallogr.* **1976**, *A32*, 751). From the ionic radius of transition metal ions in octahedral symmetry ($r(Mn^{4+}) = 0.053$ nm, $r(Co^{3+}) = 0.054$ nm, and $r(Ni^{2+}) = 0.069$ nm), the average size of transition metal ions in the $[Mn_{1/3}Co_{1/3}Ni_{1/3}]O_2$ layers was calculated as 0.059 nm. The ionic radius of oxygen ion is 0.14 nm. Thus, the thickness of the $[Mn_{1/3}Co_{1/3}Ni_{1/3}]O_2$ monolayer was determined as 0.56 nm.
60. Gao, Q.; Giraldo, O.; Tong, W.; Suib, S. L. Preparation of Nanometer-Sized Manganese Oxides by Intercalation of Organic Ammonium Ions in Synthetic Birnessite OL-1. *Chem. Mater.* **2001**, *13*, 778–786.
61. Ida, S.; Ogata, C.; Eguchi, M.; Youngblood, W. J.; Mallouk, T. E.; Matsumoto, Y. Photoluminescence of Perovskite Nanosheets Prepared by Exfoliation of Layered Oxides, $K_2Ln_2Ti_3O_{10}$, $KLnNb_2O_7$, and $RbLnTa_2O_7$ (Ln: Lanthanide Ion). *J. Am. Chem. Soc.* **2008**, *130*, 7052–7059.
62. Lever, A. B. P. In *Inorganic Electronic Spectroscopy*, 2nd ed.; Elsevier: Amsterdam, The Netherlands, 1984.
63. Rives, V.; Kannan, S. Layered Double Hydroxides with the Hydrotalcite-Type Structure Containing Cu^{2+}, Ni^{2+} and Al^{3+}. *J. Mater. Chem.* **2000**, *10*, 489–495.
64. Ma, R.; Liu, Z.; Takada, K.; Fukuda, K.; Ebina, Y.; Bando, Y; Sasaki, T. Tetrahedral Co(II) Coordination in α-Type Cobalt Hydroxide: Rietveld Refinement and X-ray Absorption Spectroscopy. *Inorg. Chem.* **2006**, *45*, 3964–3969.
65. Wang, L.; Omomo, Y.; Sakai, N.; Fukuda, K.; Nakai, I.; Ebina, Y.; Takada, K.; Watanabe, M.; Sasaki, T. Fabrication and Characterization of Multilayer Ultrathin Films of Exfoliated MnO_2 Nanosheets and Polycations. *Chem. Mater.* **2003**, *15*, 2873–2878.
66. Manga, K. K.; Zhou, Y.; Yan, Y.; Loh, K. P. Multilayer Hybrid Films Consisting of Alternating Graphene and Titania Nanosheets with Ultrafast Electron Transfer and Photoconversion Properties. *Adv. Funct. Mater.* **2009**, *19*, 1–6.
67. Schaak, R. E.; Mallouk, T. E. Prying Apart Ruddlesden-Popper Phases: Exfoliation into Sheets and Nanotubes for Assembly of Perovskite Thin Films. *Chem. Mater.* **2000**, *12*, 3427–3434.
68. Wang, L. Z.; Sasaki, T.; Ebina, Y.; Kurashima, K.; Watanabe, M. Fabrication of Controllable Ultrathin Hollow Shells by Layer-by-Layer Assembly of Exfoliated Titania Nanosheets on Polymer Templates. *Chem. Mater.* **2002**, *14*, 4827–4832.
69. Wang, L.; Takada, K.; Kajiyama, A.; Onoda, M.; Michiue, Y.; Zhang, L.; Watanabe, M.; Sasaki, T. Synthesis of a Li−Mn−oxide with Disordered Layer Stacking through Flocculation of Exfoliated MnO_2 Nanosheets, and Its Electrochemical Properties. *Chem. Mater.* **2003**, *15*, 4508–4514.
70. Suzuki, S.; Miyayama, M. Lithium Intercalation Properties of Octatitanate Synthesized through Exfoliation/Reassembly. *J. Phys. Chem. B* **2006**, *110*, 4731–4734.
71. Suzuki, S.; Miyayama, M. Lithium Intercalation Properties of Reassembled Titanate/Carbon Composites. *J. Electrochem. Soc.* **2007**, *154*, A438–443.
72. Kang, J. H.; Paek, S. M.; Hwang, S. -J.; Choy, J. -H. Pre-swelled Nanostructured Electrode for Lithium Ion Battery: TiO_2-Pillared Layered MnO_2. *J. Mater. Chem.* **2010**, *20*, 2033–2038.